Transport and Binding of Methotrexate *In Vivo*

R. L. DEDRICK*▲, D. S. ZAHARKO†, and R. J. LUTZ*

Abstract □ A mathematical model is presented for time-dependent uptake of drugs in tissues exhibiting significant membrane resistance to transport during periods of rapidly changing plasma concentration *in vivo*. The model includes joint effects of blood flow, membrane transport, and binding. It is used to interpret data on the uptake of methotrexate in bone marrow, spleen, and small intestine of the bile-cannulated rat following intravenous doses of 0.05, 0.25, 2.5, and 25 mg./kg. The transport is saturable and influenced by strong intracellular binding. The Michaelis constant ranges from 0.45 mcg./ml. (1.0 μM) to 1.1 mcg./ml. (2.4 μM), in general agreement with *in vitro* studies in a number of mammalian cell lines.

Keyphrases □ Methotrexate—*in vivo* transport and binding, mathematical model for time-dependent uptake in tissues, rats □ Transport parameters, *in vivo* methotrexate—mathematical consideration of blood flow, membrane permeability, and binding □ Tissue distribution, *in vivo* methotrexate, rats—transport parameters, mathematical model for time-dependent uptake □ Drug transport —mathematical model for time-dependent uptake in tissues during rapidly changing plasma concentration *in vivo*

The mechanism of action of methotrexate[1] has been reviewed by Bertino and Johns (1). It is a strong inhibitor of the enzyme dihydrofolate reductase, which catalyzes the formation of tetrahydrofolate. DNA synthesis is inhibited if tetrahydrofolate is not available for the production of a coenzyme required for thymidylate formation. Additional sites of action have been proposed, which complicate the complete description of the biochemical events leading to cell death or recovery following exposure to methotrexate.

Methotrexate can be highly toxic to rapidly proliferating normal cells because it kills cells in S-phase (the DNA synthetic phase). Therapeutic application of methotrexate to a tumor-bearing host exposes both tumor and sensitive normal cells to the drug at concentrations and with time courses determined jointly by the dose schedule, route of administration, and physiological disposition. The therapeutic framework must be optimized so that tumor cells are destroyed more rapidly than they are produced, with constraints imposed by toxicity to the host. Within this framework, rather subtle differences in cell kinetics, drug transport, and tissue perfusion may be exploited despite the rather general biochemical mechanism of action.

Defective membrane transport has been proposed as a mechanism of drug resistance in the murine leukemia L5178Y (2). Drug transport has been associated with sensitivity or resistance of a number of other tumors including the Yoshida sarcoma in rats (3, 4), P-388 leukemia in mice (5), Ehrlich ascites tumor (6), a variety of mouse leukemias (7), human leukemia (8), and mouse L-1210 leukemia (9).

Transport of methotrexate into mammalian tumor cells has been studied extensively *in vitro*. A few studies in addition to those already cited include the mouse L-1210 leukemia (10–13) and Sarcoma-180 (14, 15). Werkheiser (16) studied the uptake of methotrexate by ascitic P-388 leukemia in mice. A number of aspects of methotrexate transport in mammalian cells were discussed by Goldman (17). Werkheiser (18) also developed a theoretical mathematical model which includes the effect of finite permeability on the action of methotrexate *in vivo*. Data on rates of diffusion of methotrexate into sensitive normal tissues *in vivo* have not been published. Past investigations of the distribution of methotrexate *in vivo* (19, 20) indicated that blood flow and protein binding could not explain the rate of uptake in bone marrow, the spleen, and the GI tract. That these are important sites of action is suggested by clinical findings of leukopenia, thrombocytopenia, and intestinal toxicity (21).

The purposes of this paper are: (*a*) to report transport parameters for entry of methotrexate into bone marrow, the small intestine, and the spleen of the rat and (*b*) to present a mathematical model for the interpretation of the observed uptake during time intervals in which the plasma concentration is decreasing rapidly because of drug redistribution and elimination. Data were obtained following pulse intravenous injections at four doses ranging from 0.05 to 25 mg./kg. A mathematical model has been developed to incorporate the joint effects of blood flow, transport across cell membranes, and strong intracellular binding (presumed to be due to dihydrofolate reductase). The mathematical treatment is general and can be adapted to other normal tissues or to tumors in which blood flow, membrane permeability, and binding must be considered together.

EXPERIMENTAL

The concentration of methotrexate in the various tissues of the rat was obtained as follows. The tritiated drug, 3′,5′,9-^{3}H-methotrexate[2], in chromatographically pure form (22) was mixed with nonlabeled drug[3] dissolved in 2% sodium bicarbonate. Each animal received an injection into the femoral vein of 0.001 ml. labeled methotrexate solution/g. body weight; radioactivity (3–9 μc./kg.) was sufficient to give tissue levels with counting errors of 5% or less. Doses ranged from 0.05 to 25 mg./kg.

[1] *N* - [*p* - [(2,4 - Diamino - 6 - pteridinylmethyl)methylamino]benzoyl] glutamic acid. Methotrexate is currently used in the treatment of leukemia and other tumors.

[2] New England Nuclear.
[3] NCS 740, Lederle.

The rats were anesthetized with pentobarbital (60 mg./kg. i.p.) and maintained at a reflex-free level of anesthesia by supplementary doses as necessary. A midline laparotomy was performed, and the bile duct was cannulated with polyethylene 20 tubing. Control bile was collected until a constant flow of 20 μl./min. was achieved. Body temperature was maintained at 36 ± 0.5° throughout the experiment by a heating lamp and monitored constantly with a thermistor-type rectal thermometer[4].

The animals were decapitated at selected times after injection of methotrexate and tissue samples were collected. The entire small intestine minus expressible contents was homogenized as were the spleen and other tissues; the bone marrow from two femurs was removed by cracking open the bones and aspirating the contents into a tared micropipet; the blood was centrifuged to collect plasma. Aliquots of the tissue homogenates, plasma, and the entire sample of bone marrow were combusted and counted (23). The counts were converted to micrograms of drug per unit of tissue after appropriate corrections for quenching, volumes, and weights of tissues.

As reported previously, significant metabolism of methotrexate by intestinal bacteria occurs in rats after 6 hr. (24). With this consideration in mind, the comparison of model predictions with experimental data was limited to short times so that the tritium measured actually represents intact drug.

The diversion of the bile from the intestinal lumen made it possible to analyze the rate of methotrexate uptake into the small intestine from the vascular compartment without the complication of enterohepatic recirculation.

In those studies in which extracellular space of tissues was determined by inulin-^{14}C, the same experimental procedure as already described was used. Inulin-^{14}C[2] in 0.1 *M* phosphate buffer at pH 7.0 was the injection fluid. The inulin-^{14}C was purified just prior to use by a Sephadex chromatography procedure (25).

DEVELOPMENT OF MODEL

A mathematical model has been published which simulates the distribution and disposition of methotrexate in several mammalian species (19, 26) and in the sting ray (20). Since this model and its key assumptions were described previously, only a summary development is presented here. Careful attention is given to the operational formulation of transport within a region which may be influenced by membrane transport as well as flow.

Scheme I is a flow diagram showing the compartments in the mathematical model. The spleen and marrow compartments are small and contribute little to the systemic distribution of methotrexate, but they are included because they are important sites of action for the drug. This scheme differs from the previously published diagram in a number of ways. The bile is led directly out of the common bile duct. Diversion of the bile minimizes drug metabolism and eliminates the enterohepatic circulation. With this experimental design, reabsorption kinetics, which are not well quantified in the intact rat, are not required in the model. In addition, elimination of bile secretion into the contents of the small intestine provided the opportunity to observe transport directly between blood and gut tissue with a greatly reduced role of luminal drug contents in obscuring pharmacokinetic events in the tissue.

A skin compartment has been included, which contributes more to the distribution of the drug than had been previously realized and which serves to maintain elevated plasma concentrations at long times, since it is poorly perfused.

The bone marrow, spleen, and GI compartments include a detailed representation of drug transport across the cell membrane. Although bone marrow and spleen are small and play no significant role in influencing the systemic drug distribution, analysis of their kinetic behavior is important. Transport within the GI tract, the bone marrow, and the spleen shows time-dependent behavior that is quite different from the apparent flow limitation observed for a number of other tissues. This suggests a more complex process involving a significant role of cell membranes in determining the rate of drug uptake by these tissues.

A mass-balance equation is written for each compartment in the mathematical model. The resulting set of differential equations is solved simultaneously to simulate the concentration of drug in each compartment as a function of time. For example, the balance equation on the kidney is:

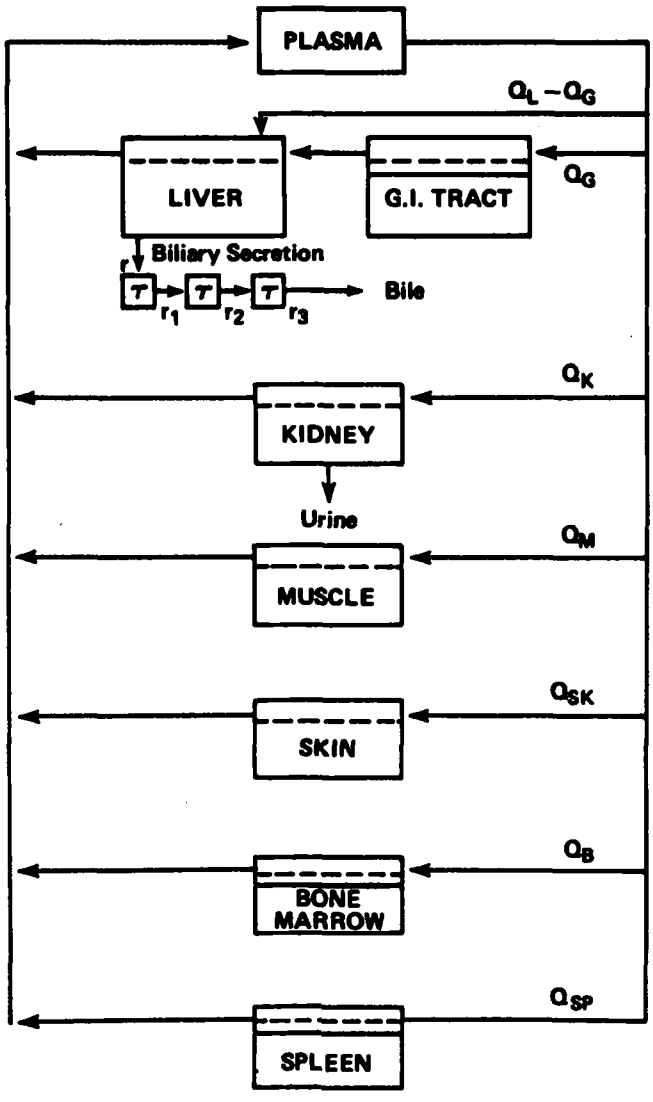

Scheme I—Diagram of compartmental model for bile-cannulated rat, where Q represents plasma flow rate to various compartments (milliliters per minute), r represents rate of flow of drug in bile (micrograms per minute), and τ represents the bile transport parameter (minutes). Values of these parameters are given in Table I.

$$V_K \frac{dq_K}{dt} = Q_K \left(q_p - \frac{q_K}{R_K}\right) - k_K \frac{q_K}{R_K} \qquad \text{(Eq. 1)}$$

where:

- Q = plasma flow rate, grams per minute or milliliters per minute
- V = size of compartment, grams or milliliters
- q = total (free plus bound) concentration in the tissue, micrograms per gram or micrograms per milliliter
- k = "clearance" (defined by Eq. 1), milliliters per minute
- R = equilibrium tissue-to-plasma distribution ratio, $(q/q_p)_{eq}$
- t = time, minutes

and the subscript, K, identifies the compartment.

The rate of flow of drug in the urine from the kidney at any time is: $k_K(q_K/R_K)$, and the cumulative amount of drug in the urine is:

$$U = \int_0^t k_K \frac{q_K}{R_K} d\tau \qquad \text{(Eq. 2)}$$

Implicit in Eq. 1 is the assumption of flow limitation in the sense that the plasma leaving the compartment is in equilibrium with the compartment so that a thermodynamic distribution ratio can be used. This idea is inferred from Fig. 1, in which the concentrations

[4] Yellow Springs Instrument Co.

Table I—Model Parameters for 200-g. Rat

Parameter	Compartment											
						Gut		Spleen		Bone Marrow		
	Plasma	Muscle	Kidney	Liver	Skin	ECF[a]	ICF[a]	ECF[a]	ICF[a]	ECF[a]	ICF[a]
Volume, ml.	9.0	100.0	1.9	8.3	35.0[b]	11.0		0.54[c]		4.0[d]	
V						3.7	7.3	0.11	0.43	0.80	3.2
Flow rate, ml./min.	22.7	3.0	5.0	6.5	2[e]	5.3	—	0.25[e]	—	0.64[f]	—
Q											
Linear distribution ratio	—	0.15	3.0	3.0	1.0	—	—	—	—	—	—
R											
Strong binding constant, mcg./ml.	0	0	0.3	0.5	0	0	0.2	0	0.1	0	0.2
a'											
Dissociation constant, mcg./ml.	—	—	0.00001	0.00001	—	—	0.00001	—	0.00001	—	0.00001
ϵ											
"Clearance," ml./min.	—	—	2.0	5.7	—	—	—	—	—	—	—
Bile transit parameter, min.	—	—	—	1.0	—	—	—	—	—	—	—
τ											
Maximum facilitated transport, mcg./(min.)(ml.)	—	—	—	—	—	0.014		0.009		0.012	
k											
Michaelis constant, mcg./ml.	—	—	—	—	—	0.45		1.1		0.9	
K											

[a] ECF = extracellular fluid, and ICF = intracellular fluid. [b] Jansky and Hart (32). [c] *Reference 33.* [d] Mapleson (34), ratioed to 200-g. rat. [e] Mandel and Saperstein (35), for 45% hematocrit. [f] Brookes (36).

in the liver, kidneys, and skeletal muscles of mice are plotted as functions of the plasma concentration. Time does not appear explicitly in this plot. An intermediate point on the curve may have been obtained at a short time following a small dose or after a longer time following a larger dose. This suggests that (on the time scale of the experiments at least) a unique relationship exists between the plasma concentration and the concentration in each of these three tissues. Distribution into muscle is linear, and the volume of distribution is approximately equal to the extracellular fluid volume. At high plasma concentrations, the drug is concentrated in the liver and kidneys about 10:1 and 3:1, respectively. At low plasma concentrations, these tissue concentrations appear to approach constant values presumed to be associated with strong binding of methotrexate to dihydrofolate reductase. *In vivo* binding isotherms, therefore, consist of a linear part and a saturable part with a very low dissociation constant, and the distribution coefficients are functions of plasma concentration.

If the concentrations in the bone marrow, the spleen, and the small intestine are plotted in the manner of Fig. 1, no unique thermodynamic relationship is seen between the drug in the tissue and that in the plasma. This is illustrated for bone marrow in Fig. 2. The dependence of the concentration of drug in the tissue on dose (and thus prior drug exposure) as well as on plasma concentration suggests an analysis which includes membrane resistance to transport. The mathematical analysis presented here is rather general and can be applied or easily adapted to any lumped compartment in which flow, membrane transport, and binding must be considered jointly. It is developed in some detail with explicit citation of model assumptions.

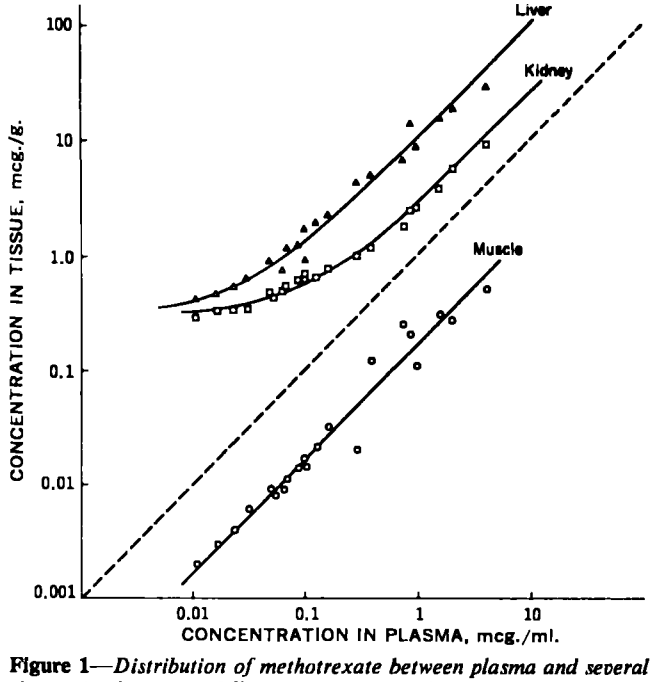

Figure 1—*Distribution of methotrexate between plasma and several tissues in the mouse following intravenous doses of 0.1, 0.3, and 3 mg./kg. at times from 5 to 120 min.*

General Balance Equations—A mass balance on each section of the compartment in Scheme II gives:

$$V_1\frac{dq_1}{dt} = Q(q_p - q_1) - (jA)_{12} \qquad \text{(Eq. 3)}$$

$$V_2\frac{dq_2}{dt} = (jA)_{12} - (jA)_{23} \qquad \text{(Eq. 4)}$$

$$V_3\frac{dq_3}{dt} = (jA)_{23} \qquad \text{(Eq. 5)}$$

where j = net flux of drug, mcg./(min.)(cm.^{2}); A = area for transport, cm.^{2}; and the single subscripts 1, 2, and 3 refer to plasma, interstitial fluid, and intracellular fluid, respectively. The double subscripts 12 and 23 indicate the directions shown in the scheme. The flux, j, and the area, A, are defined separately here; however, values were not obtained for each. Their product is treated as a single concept (rate of transport) as is common practice in both physiology and engineering. If an independent measure of the area becomes available, the actual fluxes can be calculated.

Binding—In each compartment, the total concentration is given as the sum of the free and the bound concentration:

$$q_j = f_jC_j + (1 - f_j)x_j \qquad j = 1, 2, 3 \qquad \text{(Eq. 6)}$$

with:

$$x_j = x_j(C_j) \qquad j = 1, 2, 3 \qquad \text{(Eq. 7)}$$

where:

- f_j = fraction of water in the jth compartment
- C_j = free concentration, micrograms per gram or micrograms per milliliter
- x_j = bound concentration based on $(1 - f_j)$, micrograms per gram or micrograms per milliliter

In the intracellular compartment there may be both linear nonspecific binding to proteins and other cellular constituents (B_3C_3) and strong specific binding to dihydrofolate reductase (a_3C_3)/($\epsilon_3 + C_3$), where a_3 is the strong binding capacity and ϵ_3 is the dissociation constant of the drug–enzyme complex. Thus, the total

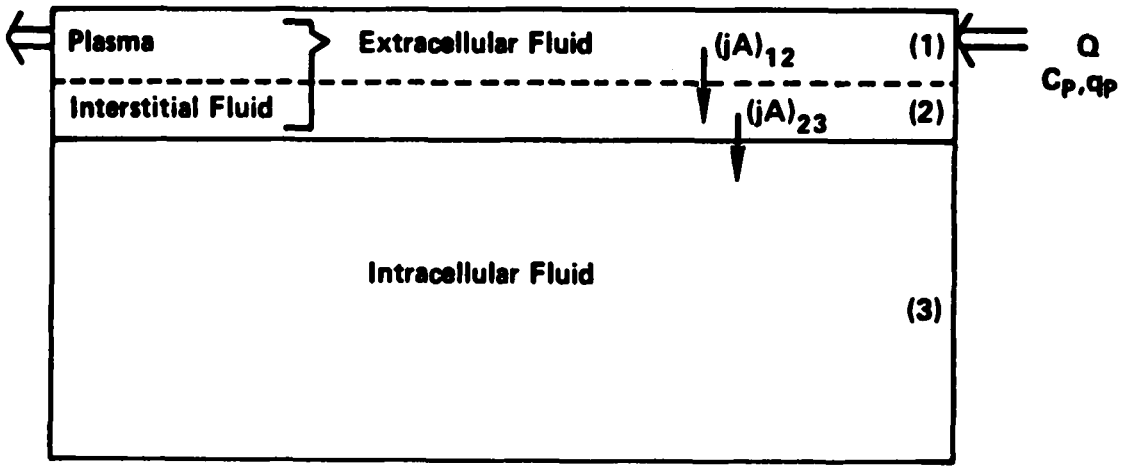

Scheme II—Diagram of a compartment (e.g., *bone marrow*) *which shows inter- and intratissue drug transport, where* Q *is the plasma flow rate to the compartment* (*milliliters per minute*), C_p *is the plasma concentration of free drug* (*micrograms per milliliter*), Q_p *is the total plasma concentration of drug* (*free + bound*) (*micrograms per milliliter*), *and* (jA) *is the transmembrane rate of transport* (*micrograms per minute*).

bound concentration inside the cells is expressed as $x_3 = B_3C_3 + (a_3C_3)/(\epsilon_3 + C_3)$.

From Eq. 6, the total intracellular concentration, free plus bound, becomes:

$$q_3 = f_3C_3 + (1 - f_3)x_3 \quad \text{(Eq. 8a)}$$

$$q_3 = f_3C_3 + (1 - f_3)B_3C_3 + (1 - f_3)\frac{a_3C_3}{\epsilon_3 + C_3} \quad \text{(Eq. 8b)}$$

or:

$$q_3 = \phi_3C_3 + \frac{a_3'C_3}{\epsilon_3 + C_3} \quad \text{(Eq. 8c)}$$

where $\phi_3 \equiv f_3 + (1 - f_3)B_3$ and $a_3' \equiv (1 - f_3)a_3$.

Linear binding to plasma proteins and cell membranes may occur in the extracellular compartment, giving $x_1 = B_1C_1$ and $x_2 = B_2C_2$ so that:

$$q_1 = [f_1 + (1 - f_1)B_1]C_1 = \phi_1C_1 \quad \text{(Eq. 9)}$$

$$q_2 = \phi_2C_2 \quad \text{(Eq. 10)}$$

The previous equations can be simplified by assuming that the linear protein binding terms in all compartments are small[6]. Then B_1, B_2, $B_3 \approx 0$; f_1, f_2, $f_3 \approx 1$; and ϕ_1, ϕ_2, $\phi_3 \approx 1$. From Eqs. 8–10, the total concentration in each compartment is now:

$$q_1 = C_1 \quad \text{(Eq. 11)}$$

$$q_2 = C_2 \quad \text{(Eq. 12)}$$

$$q_3 = C_3 + \frac{a_3'C_3}{\epsilon_3 + C_3} \quad \text{(Eq. 13)}$$

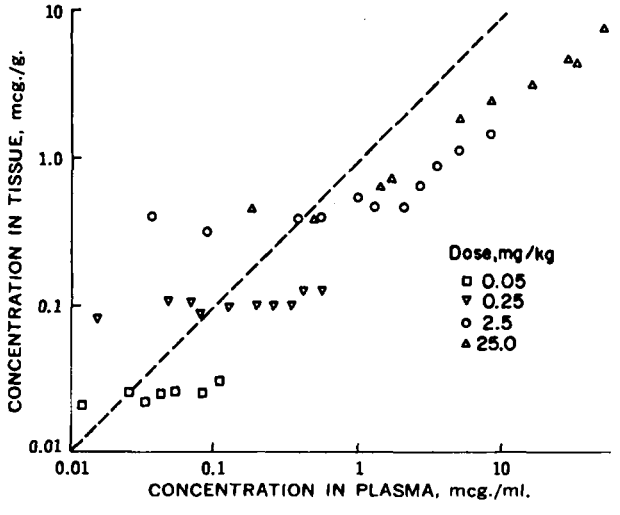

Figure 2—*Distribution of methotrexate between plasma and bone marrow of the rat at several doses.*

[6] The binding of methotrexate to rat plasma is about 15%.

Transport—It is assumed that the rate of transport, $(jA)_{13}$, is very fast, *i.e.*, very rapid equilibration across the capillary membrane so that plasma leaving the compartment and interstitial fluid have the same concentration at all times: $C_1 = C_2 = C_e$ and $C_3 = C_i$, where the subscripts *e* and *i* refer to extracellular and intracellular, respectively. Let:

$$(jA)_{23} = \frac{kVC_e}{K + C_e} - \frac{kVC_i}{K + C_i} + bV(C_e - C_i) \quad \text{(Eq. 14)}$$

Equation 14 describes saturable transport (first two terms on right-hand side) occurring in parallel with passive transport (third term). The transport parameters k (maximum facilitated rate) and b (passive permeability) are arbitrarily based on a unit volume or weight of tissue. The Michaelis constant for transport is K. Equation 14 incorporates the assumption that the facilitated transport is symmetric in the sense that $k_e = k_i = k$ and $K_e = K_i = K$.

If one adds balance Eqs. 3 and 4 and uses Eqs. 11 and 12 with $C_1 = C_2 \equiv C_e$ and $V_e = V_1 + V_2$, one gets:

$$V_e\frac{dC_e}{dt} = Q(C_p - C_e) - (jA)_{23} \quad \text{(Eq. 15)}$$

Inserting Eq. 13 for q_3 into balance Eq. 5 with $C_3 = C_i$ and carrying out the appropriate differentiation give Eq. 16, explicit in free intracellular concentration C_i:

$$V_i\frac{dC_i}{dt} = \frac{(jA)_{23}}{1 + \epsilon_i a_i'/(\epsilon_i + C_i)^2} \quad \text{(Eq. 16)}$$

Equations 14–16 are the working forms of the equations used for computation. They require estimates of the extracellular and intracellular volumes (V_e and V_i), the plasma flow rate to the compartment (Q), the transport parameters (k, K, and b), and the binding constants (ϵ_i and a_i').

RESULTS

Table I lists the model parameters used for simulation of plasma and tissue concentrations in the rat. They include those from a previous study (19) with a few exceptions: (*a*) there was no requirement for gut–lumen parameters in the anesthetized bile-cannulated rat, (*b*) clearance of methotrexate by the kidney was increased by the anesthesia so that the kidney clearance as defined by Eq. 1 was found to be 2.0 ml./min., (*c*) the bile secretion values were revised on the basis of data from the current study, and (*d*) binding constants in the GI tract were replaced by a more complete model of transport and binding in the small intestine.

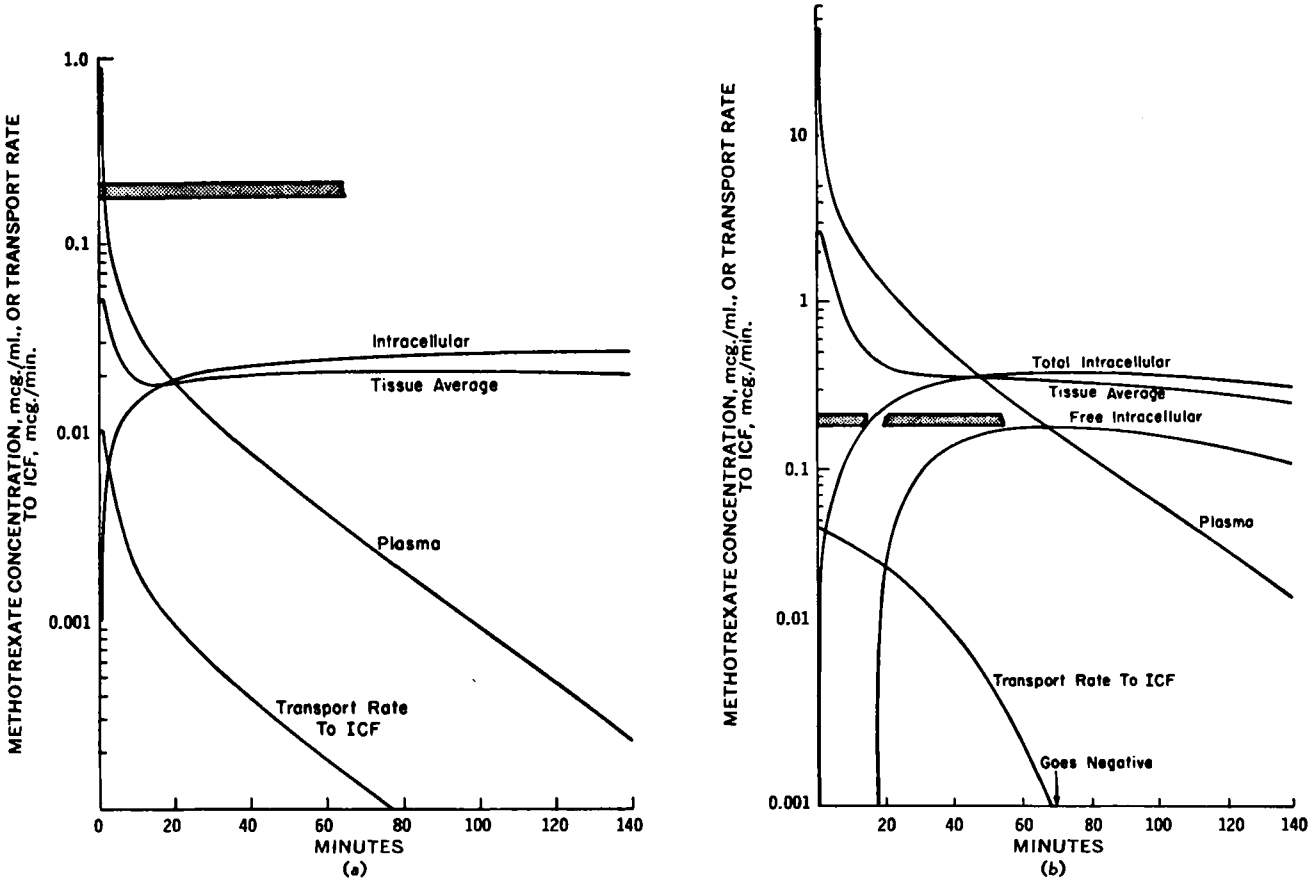

Figure 3—*Simulated plasma concentration and concentrations and transmembrane transport rate of methotrexate in bone marrow of rat. Shaded bar represents strong binding capacity, presumably dihydrofolate reductase, micrograms methotrexate per milliliter cell contents. It is assumed constant for the duration of the experiment. Key:* (a), *0.05 mg./kg. i.v.; and* (b), *2.5 mg./kg. i.v. ICF = intracellular fluid.*

As discussed previously, additional parameters were required to describe saturable transport and binding in the bone marrow, the spleen, and the small intestine and to incorporate a skin compartment. Plasma flow and volume of the skin, the spleen, and the bone marrow were obtained from the literature as documented in the table. Parameters not discussed in the previous work (19) include V_s, V_t, k, K, b, and a_t' in the compartments exhibiting time-dependent uptake. These were obtained from the data to simulate the measured time course of drug concentration in these compartments as discussed below.

Extracellular Volume (V_e)—This was first based on the tissue to plasma concentration ratio for inulin after a pulse injection. A better second estimate was obtained from tissue to plasma methotrexate ratios obtained at short times following the highest dose. Because of transport saturation under these conditions, intracellular drug appears to comprise a very small fraction of measured drug. The methotrexate extracellular "space" of 20% in the bone marrow is slightly greater than the 15% observed for inulin, a finding consistent with observations on muscle.

Intracellular Volume (V_i)—$V_i = V - V_e$.

Membrane Transport Parameters (k, K, b)—There was proportionality between the amount of drug in a tissue and dose (and area under the plasma concentration curve) at the two lowest doses. This suggests a linear transport. For a dose that does not saturate the dihydrofolate reductase in the cells, efflux is negligible. Then, from Eq. 14, with $b = 0$:

$$(jA)_{12} = \frac{kVC_e}{K + C_e} \qquad \text{(Eq. 17)}$$

and for $C_e \ll K$:

$$(jA)_{12} = \frac{kV}{K} C_e \qquad \text{(Eq. 18)}$$

The amount in the cells at any time, t, is:

$$\text{amount} = \int_0^t \frac{kV}{K} C_e d\tau \qquad \text{(Eq. 19)}$$

Since $C_t \approx C_P$, this equation provides a first estimate of the ratio k/K. The data on tissue uptake *versus* time could then be simulated within the context of the model to give a more precise estimate of k/K and of K from the data at higher doses when saturation of the transport process occurred. It was not necessary to use a finite value of the permeability to passive diffusion, b; however, a very small value cannot be ruled out on the basis of the data.

Intracellular Binding Constant (a)—Following doses thought sufficient to saturate the intracellular dihydrofolate reductase, the tissue concentration at longer times remained nearly constant after correction for extracellular drugs. This provided an initial estimate of a'. Inspection of numerous simulations provided a better estimate.

The dissociation constant (ϵ_i) for the dihydrofolate reductase-methotrexate complex was estimated from *in vitro* data of Werkheiser (27) as discussed previously (19).

Following a pulse intravenous injection of methotrexate, the plasma concentration decreases very rapidly for a few minutes, followed by a longer and slower exponential phase which results when the bile is diverted, since no significant intestinal reabsorption occurs. A dynamic and complex set of events occurs in those tissues that have a significant membrane resistance. Figures 3*a* and 3*b* illustrate these events for bone marrow at two different doses as interpreted by the model.

At 0.05 mg./kg. (Fig. 3*a*), the predicted extracellular concentration peaks very rapidly and then closely follows the predicted plasma concentration. Drug enters the intracellular compartment through the cell membranes; however, there is insufficient transport to saturate all the intracellular dihydrofolate reductase. The total marrow concentration is a weighted average of the extracellular and intracellular compartments. Since ϵ is of the order of 10^{-11} M or less (27), the free intracellular concentration remains near zero as long

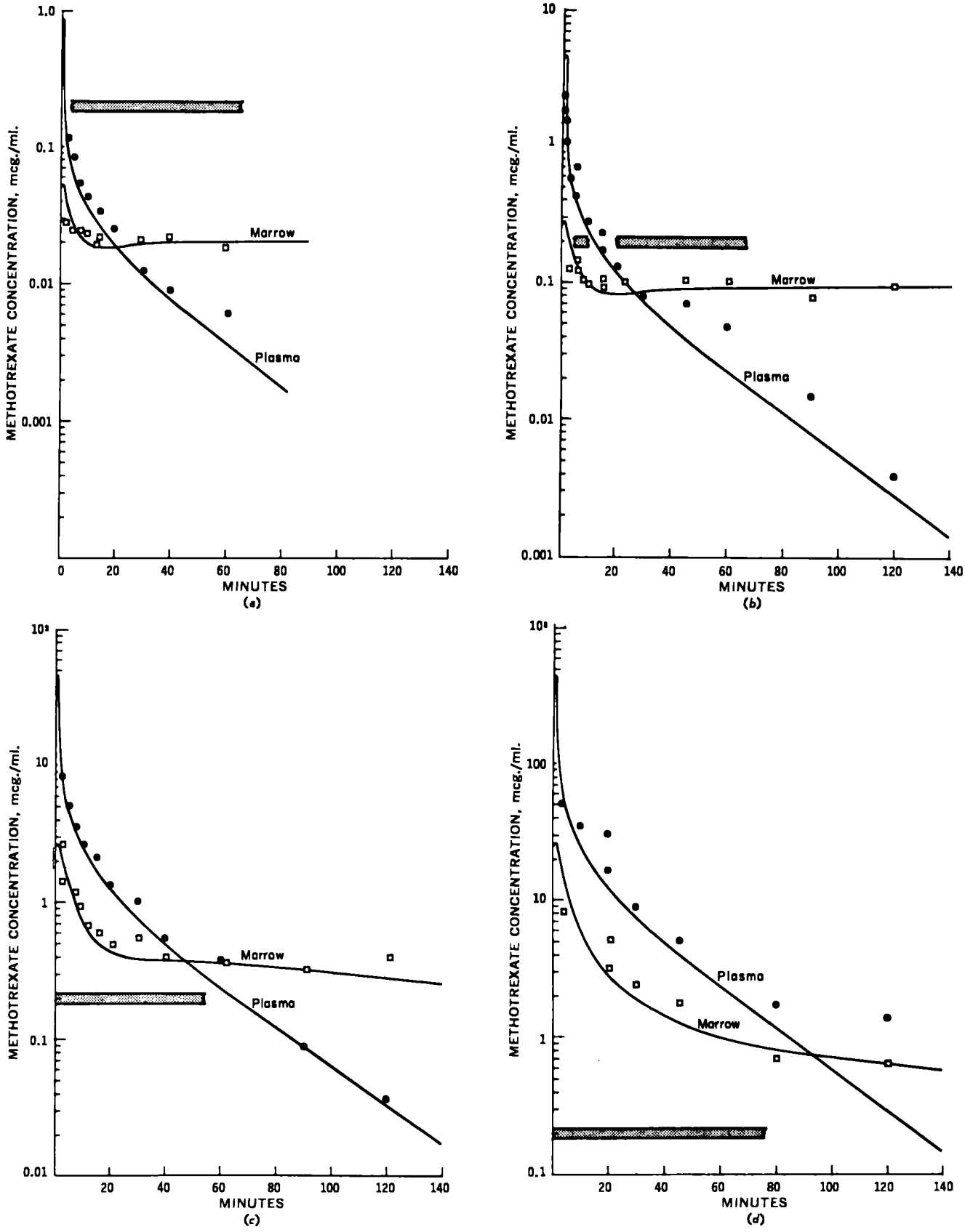

Figure 4—*Plasma and average bone marrow concentrations of methotrexate in rat. Solid lines represent model simulations. Data points were obtained from one rat at each time. Key:* (a), *0.05 mg./kg. i.v.;* (b), *0.25 mg./kg. i.v.;* (c), *2.5 mg./kg. i.v.; and* (d), *25 mg./kg. i.v.*

as free dihydrofolate reductase is available. Therefore, influx of methotrexate can occur even after the plasma concentration is less than the total intracellular concentration. It is sufficiently slow during this time interval, however, that the measured marrow concentration remains about constant.

Following a dose of 2.5 mg./kg. (Fig. 3*b*), the simulated intra-

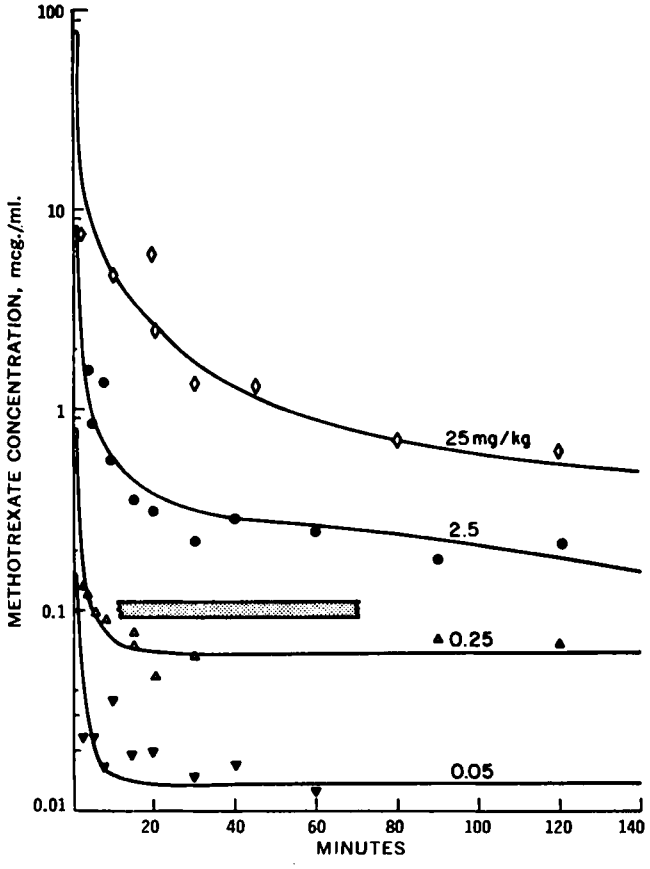

Figure 5—*Average concentrations of methotrexate in spleen of rat. Solid lines represent model simulations. Each data point was obtained from a single rat.*

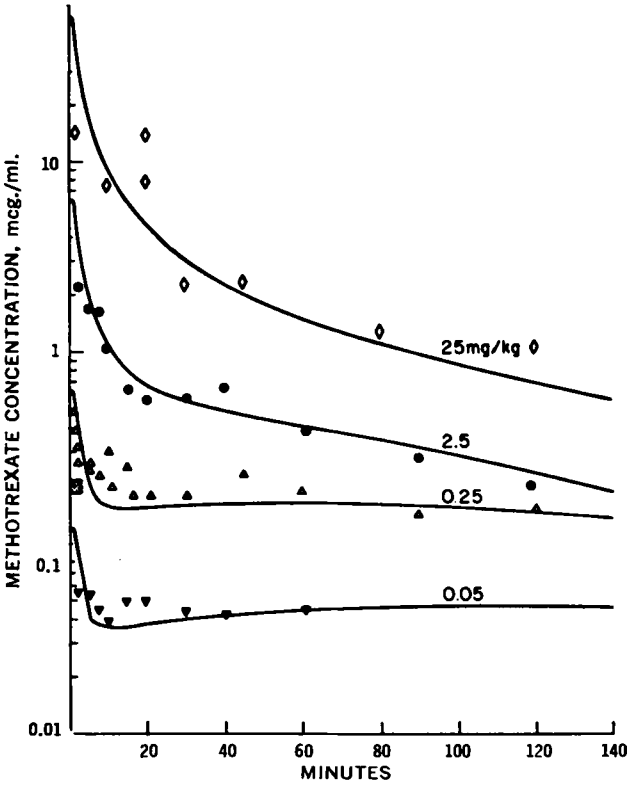

Figure 6—*Average concentrations of methotrexate in small intestine of rat with bile diverted. Solid lines represent model simulations. Each data point was obtained from a single rat.*

cellular events are somewhat different. There is sufficient entry of drug by about 20 min. to saturate the dihydrofolate reductase. At this time, there is an abrupt rise in free intracellular drug concentration. Efflux of drug occurs beyond 75 min. since the *free* intracellular drug concentration exceeds the extracellular concentration which is constantly decreasing with plasma. It is apparent that total tissue concentration is not a valid measure of intracellular drug at all times. Most of the measured drug is located extracellularly at the termination of a short experiment. In fact, washout of drug with plasma from the extracellular space makes the measured tissue concentration decrease rapidly during an early phase, even though there is actually uptake by the cells.

Figures 4*a*–4*d* compare model simulations with experimental data for bone marrow at four doses, ranging from 0.05 to 25 mg./kg. for time periods up to 2 hr. Both the shape of the bone marrow curves and their position with respect to the plasma curves change. There is a systematic variation from a relatively flat shape at the lowest dose to one exhibiting a pronounced decrease with time at the highest dose. The plasma concentration is approximately proportional to dose at all times, consistent with earlier observations (28); however, the measured marrow concentration is not. There is approximate proportionality in the marrow for a few minutes, which reflects the dominant role of extracellular fluid concentration. At longer times, increasing the dose by a factor of 5 from 0.05 to 0.25 mg./kg. increases the marrow concentration from 0.02 to 0.1 mcg./g., also a factor of 5. Since the plasma and extracellular concentrations are much lower than the total marrow concentration, these values represent intracellular drug. Further increases in dose to 2.5 and 25 mg./kg. do not result in proportional increases in marrow concentrations at long times. This behavior strongly suggests a saturable transport process. Symmetric transmembrane-facilitated diffusion with no significant passive component (Eq. 14) gave a satisfactory simulation of the data. The maximum facilitated rate (k), the Michaelis constant (K), and the methotrexate equivalent of intracellular dihydrofolate reductase (a') are given in Table I.

Figures 5 and 6 compare tissue concentrations in the spleen and small intestine with model simulations following the same four doses. The same qualitative picture exists. It may be explained by the general considerations discussed with Figs. 3*a* and 3*b*. Satisfactory transport and binding parameters are listed in Table I. These are similar for all three tissues.

DISCUSSION

A rather complex model was required to explain the observations concerning the pharmacokinetics of methotrexate in several tissues critical to its toxicity. Part of the complexity arose from the desire to simulate *in vivo* processes with changing plasma concentrations that occur after a single dose. This situation contrasts with studies *in vitro*, which have consistently been conducted at constant medium concentrations. The basic model was derived from earlier work which was shown to simulate adequately the concentrations in plasma and a number of tissues. The large number of parameters required are mostly physiological, anatomical, or physicochemical. The additional complexity involved the incorporation of saturable transport between extracellular and intracellular compartments in certain tissues. Other tissues are still satisfactorily simulated by a lumped, single compartment and flow-limited conditions.

A detailed analysis of the sensitivity of the model to each parameter was not undertaken. The model was perturbed by varying a number of parameters individually, and simulations were made to illustrate its behavior.

Figure 7 shows the necessity for saturability of the transport. If Eq. 14 is written:

$$(JA)_{23} = \frac{kV}{K} C_e - \frac{kV}{K} C_t \qquad \text{(Eq. 20)}$$

it describes transport that is linear in free concentration at all doses. The simulation is satisfactory at the lowest dose, since the plasma concentration is much less than the *in vivo* K, and essential linearity exists. At the higher doses, there is a systematic and serious deviation from the data and previous simulations.

For sufficiently high cell permeability, blood flow to a compartment becomes the limiting factor for drug transport. Figure 8

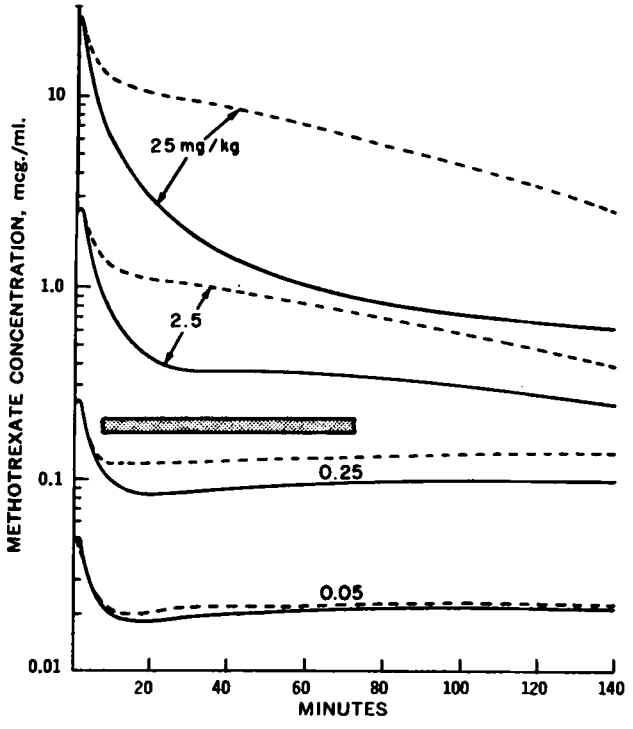

Figure 7—*Comparison of model simulation of linear and saturable transport in bone marrow at several doses. The dashed lines represent the model simulations for linear transport to the intracellular compartment of bone marrow as described by Eq. 20. The solid lines represent model simulations with saturable transport (Eq. 14).*

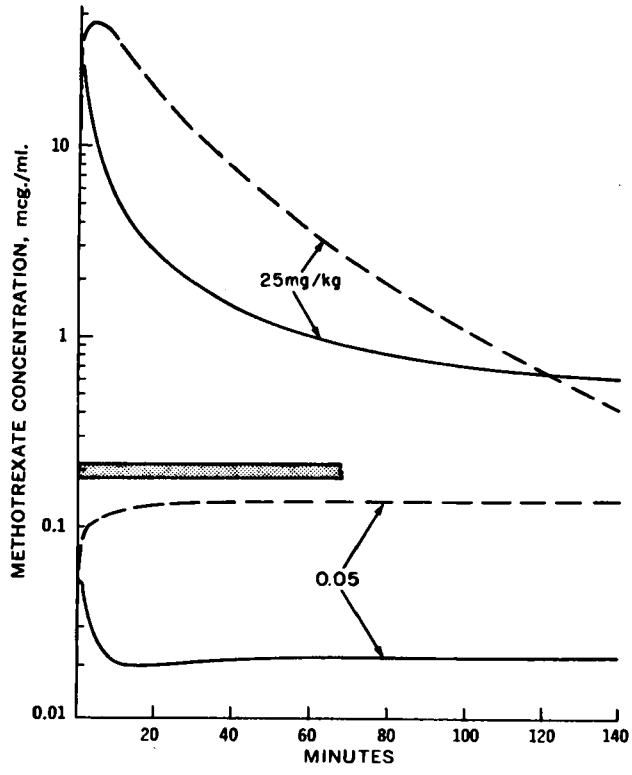

Figure 8—*Effect of very high permeability (flow limitation) on model simulations in bone marrow at two doses. The dashed lines represent bone marrow modeled as an equilibrium, flow-limited compartment. The solid lines represent model simulations with saturable transport.*

illustrates the results for a model simulation of bone marrow for this flow-limited case. There are very large deviations from previous simulations. Membrane resistance is significant if the permeability (k/K) for linear transport is much smaller than the tissue perfusion (29). For the bone marrow:

$$\frac{k}{K} = \frac{0.012 \text{ mcg./(min.)(ml.)}}{0.9 \text{ mcg./ml.}} = 0.013 \text{ min.}^{-1} \quad \text{(Eq. 21)}$$

which is much less than the plasma flow rate per unit volume:

$$\frac{Q}{V} = 0.16 \text{ min.}^{-1} \quad \text{(Eq. 22)}$$

Comparable values for the other tissues are: spleen, $(k/K) = 0.0082$ min.$^{-1}$, $(Q/V) = 3.3$ min.$^{-1}$; and small intestine, $(k/K) = 0.031$ min.$^{-1}$, $(Q/V) = 0.48$ min.$^{-1}$.

The plasma flow rates to the bone marrow, the spleen, and the small intestine are estimates based on the literature already cited. No attempt was made to measure these parameters under the actual conditions of anesthesia used in these experiments. The type and duration of anesthesia may have some effect on blood flow to these tissues; however, the calculated values of the transport parameters k and K are not highly sensitive to blood flow in very well-perfused tissues. Any possible effect of anesthesia on k or K is unknown.

As a final simulation, the strong binding parameter, a', for bone marrow was changed from 0.2 mcg./g. to zero or 2.0 mcg./g. The resulting marrow concentrations are compared with previous simulations in Fig. 9. The high level of binding does not affect the results at the two lowest doses, since the dihydrofolate reductase would not be expected to saturate at 0.2 mcg./g. methotrexate equivalent so that free intracellular concentration remains near zero. The higher value of a' shows a marked effect at the highest dose, because the drug that enters the cell is effectively trapped and is not free to be transported out during the experiment. Setting a' equal to zero has a profound effect at the low doses, because now intracellular drug can be transported out rather than remain bound to the intracellular enzyme.

No valid comparison can be made at present between the strong binding parameter and some independent measure of dihydrofolate reductase content. For reference, strong binding in mouse and rat kidney and liver is in the range of 0.3–0.5 mcg./g. of tissue *in vivo*. Attempts to extract the dihydrofolate reductase and quantitate it *in vitro* would raise questions about both recovery and activity in the intracellular environment. The spleen, the bone marrow, and the small intestine were assayed for methotrexate for up to 2 days following doses of 2.5 and 25 mg./kg. to obtain independent data on strong binding in these tissues. At the lower dose, the amount of strong binding observed experimentally was approximately the same as the strong binding parameter used in the model, although significant scatter of the data was observed. Agreement was poor after the higher dose, and the scatter was much worse. These long time data are not proper validation of the strong binding at short times, because there can be significant synthesis of new enzyme and loss of drug-bound enzyme due to cell turnover on a time scale of 2 days. This problem is even more acute following the administration of a cytotoxic drug, which has been shown to induce cell death and increase enzyme activity (30, 31).

The transport process was modeled as symmetric facilitated diffusion (Eq. 14 with $b = 0$). The data *in vivo* do not permit a rigorous assertion that the efflux parameters k and K are identical to the corresponding influx parameters. Goldman *et al.* (11) reported different values for the influx and efflux processes in the L-1210 cell *in vitro*. Neither do the data prove that b cannot be a small positive number so that passive diffusion may be a factor at very high doses.

The Michaelis constants obtained during this work *in vivo* range from 0.45 mcg./ml. (small intestine) to 1.1 mcg./ml. (spleen). This narrow range implies that the transport mechanism may be the same for all three tissues. In fact, the values are very similar to those observed during *in vitro* experiments with a number of cell lines: 0.20–0.59 mcg./ml. for three lines of L-1210 leukemia (9), 1.8 mcg./ml. for entry of methotrexate into L-1210 cells (10), and 0.9 mcg./ml. for entry of methotrexate into rabbit reticulocytes (17).

The concepts incorporated in this model are necessary to elucidate transport processes occurring *in vivo*. Blood flow, saturable membrane transport, and complex binding can be examined jointly, and the effect of any one can be interpreted within a formal and operational context.

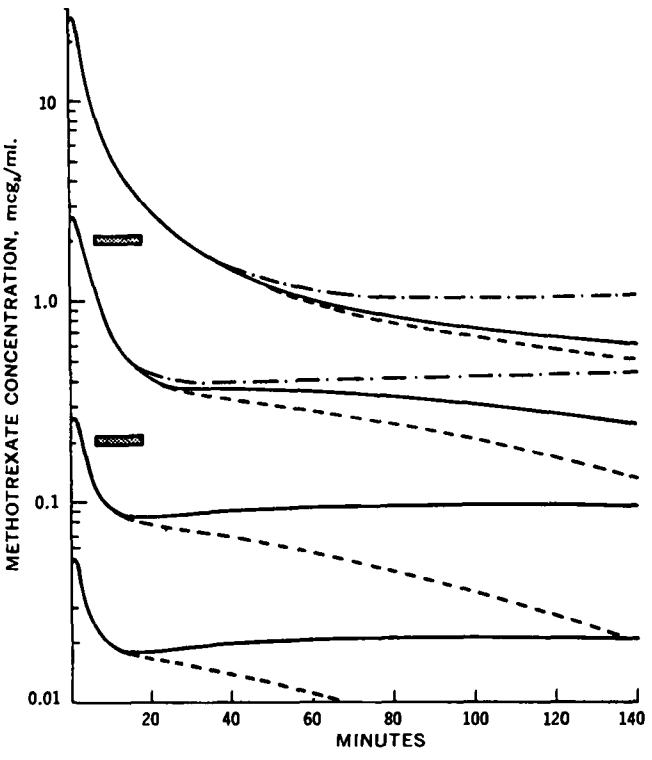

Figure 9—*Effect of change in dihydrofolate reductase content, a' (micrograms methotrexate equivalent per milliliter cell contents), on model simulations in bone marrow of rat. Key: - - -, a' = 0; —·—, a' = 2; and ——, a' = 0.2.*

While the several concepts are necessary, they may not always be sufficient. The model compartments are considered uniform in their description and behavior. No attempt was made to incorporate nonuniformities in flow. Neither was the problem of intratissue variations in the thermodynamics of binding or kinetic characteristics addressed explicitly. All of the tissues in which significant membrane limitation to transport was observed are microscopically heterogeneous. Bone marrow, for example, contains a variety of cell types in various stages of differentiation and maturity. It is probable that this distribution is accompanied by a distribution in numerous biochemical characteristics of the cells so that transmembrane transport rates and details of binding vary among the cells. Measured parameters, thus, are averages. They should not be assumed to be appropriate for every cell or even cell type within a tissue. Nevertheless, they can provide substantial pharmacokinetic insight and estimates of average local environment at appropriate biochemical sites of action.

REFERENCES

(1) J. R. Bertino and D. G. Johns, in "Cancer Chemotherapy II, The Twenty-Second Hahnemann Symposium," I. Brodsky, S. B. Kahn, and J. H. Moyer, Eds., Grune & Stratton, New York, N. Y., 1972, pp. 9–21.

(2) G. A. Fischer, *Biochem. Pharmacol.*, **11**, 1233(1962).

(3) A. Y. Divekar, N. R. Vaidya, and B. M. Braganca, *Biochim. Biophys. Acta*, **135**, 927(1967).

(4) B. M. Braganca, A. Y. Divekar, and N. R. Vaidya, *ibid.*, **135**, 937(1967).

(5) W. C. Werkheiser, L. W. Law, R. A. Roosa, and C. A. Nichol, *Proc. Amer. Ass. Cancer Res.*, **4**, 71(1963).

(6) D. Kessel and T. C. Hall, *Cancer Res.*, **27**, 1539(1967).

(7) D. Kessel, T. C. Hall, D. Roberts, and I. Wodinsky, *Science*, **150**, 752(1965).

(8) D. Kessel, T. C. Hall, and D. Roberts, *Cancer Res.*, **28**, 564 (1968).

(9) F. M. Sirotnak, S. Kurita, and D. J. Hutchison, *ibid.*, **28**, 75(1968).

(10) I. D. Goldman, *J. Biol. Chem.*, **244**, 3779(1969).

(11) I. D. Goldman, N. S. Lichtenstein, and V. T. Oliverio, *ibid.*, **243**, 5007(1968).

(12) N. S. Lichtenstein and I. D. Goldman, *Biochem. Pharmacol.*, **19**, 1229(1970).

(13) I. D. Goldman, *Biochim. Biophys. Acta*, **233**, 624(1971).

(14) M. T. Hakala, *ibid.*, **102**, 198(1965).

(15) *Ibid.*, **102**, 210(1965).

(16) W. C. Werkheiser, *Cancer Res.*, **25**, 1608(1965).

(17) I. D. Goldman, *Ann. N. Y. Acad. Sci.*, **186**, 400(1971).

(18) W. C. Werkheiser, *ibid.*, **186**, 343(1971).

(19) K. B. Bischoff, R. L. Dedrick, D. S. Zaharko, and J. A. Longstreth, *J. Pharm. Sci.*, **60**, 1128(1971).

(20) D. S. Zaharko, R. L. Dedrick, and V. T. Oliverio, *Comp. Biochem. Physiol.*, **42A**, 183(1972).

(21) H. H. Hansen, O. S. Selawry, J. F. Holland, and C. B. McCall, *Brit. J. Cancer*, **25**, 298(1971).

(22) V. T. Oliverio, *Anal. Chem.*, **33**, 263(1961).

(23) J. I. Peterson, F. Wagner, S. Siegel, and W. Nixon, *ibid.*, **31**, 189(1969).

(24) D. S. Zaharko and V. T. Oliverio, *Biochem. Pharmacol.*, **19**, 2923(1970).

(25) S. R. Cohen, *Anal. Biochem.*, **31**, 539(1969).

(26) K. B. Bischoff, R. L. Dedrick, and D. S. Zaharko, *J. Pharm. Sci.*, **59**, 149(1970).

(27) W. C. Werkheiser, *J. Biol. Chem.*, **236**, 888(1961).

(28) R. L. Dedrick, K. B. Bischoff, and D. S. Zaharko, *Cancer Chemother. Rep.*, **54**, 95(1970).

(29) R. L. Dedrick and K. B. Bischoff, *Chem. Eng. Progr. Symp. Ser. No. 84*, **64**, 32(1968).

(30) J. Borsa, G. F. Whitmore, F. A. Valeriote, D. Collins, and W. R. Bruce, *J. Nat. Cancer Inst.*, **42**, 235(1969).

(31) J. R. Bertino, A. R. Cashmore, and B. L. Hillcoat, *Cancer Res.*, **30**, 2372(1970).

(32) L. Jansky and J. S. Hart, *Can. J. Physiol. Pharmacol.*, **46**, 653(1968).

(33) "The Rat—Data and Reference Tables for Albino Rat and Norway Rat," H. H. Donaldson, Ed., Wistar Institute of Anatomy and Biology, Philadelphia, Pa., 1924, p. 212.

(34) W. W. Mapleson, *J. Appl. Physiol.*, **18**, 197(1963).

(35) M. Mandel and L. Saperstein, *Circ. Res.*, **10**, 807(1962).

(36) M. Brookes, *J. Anat.*, **101**, 533(1967).

ACKNOWLEDGMENTS AND ADDRESSES

Received October 10, 1972, from the • *Biomedical Engineering and Instrumentation Branch, Division of Research Services*, and the † *Laboratory of Chemical Pharmacology, National Cancer Institute, National Institutes of Health, Public Health Service, Department of Health, Education, and Welfare, Bethesda, MD 20014*

Accepted for publication January 16, 1973.

The authors thank Ann Peale for technical assistance in the performance of the experimental investigation.

▲ To whom inquiries should be directed.